Chapter 35
NDE of Additively Manufactured Parts via Directly Bonded and Mechanically Attached Electromechanical Impedance Sensors

C. Tenney, M. Albakri, C. B. Williams, and P. Tarazaga

Abstract Additive Manufacturing (AM) allows increased complexity which poses challenges to quality-control (QC) and non-destructive evaluation (NDE) of manufactured parts. The lack of simple, reliable, and inexpensive methods for NDE of AM parts is a significant obstacle to wider adoption of AM parts.

Electromechanical impedance measurements have been investigated as a means to detect manufacturing defects in AM parts. Impedance-based NDE utilizes piezoelectric wafers as collocated sensors and actuators. Taking advantage of the coupled electromechanical characteristics of piezoelectric materials, the mechanical characteristics of the part under test can be inferred from the electrical impedance of the piezoelectric wafer. Previous efforts have used piezoelectric wafers bonded directly to the part under test, which imposes several challenges regarding the applicability and robustness of the technique. This paper investigates the use of an instrumented clamp as a solution for measuring the electromechanical impedance of the part under test. The effectiveness of this approach in detecting manufacturing defects is compared to directly bonded wafers.

Keywords Electromechanical Impedance · Non-Destructive Evaluation · Additive Manufacturing · Piezoelectrics · Manufacturing Defects

35.1 Introduction

Additive Manufacturing (AM) processes' layer-wise approach to fabrication provides a means to greatly increase part complexity and thus functionality. However, this added geometric complexity also poses challenges to quality-control (QC) and non-destructive evaluation (NDE) of manufactured parts. Current methods, such as x-ray computed tomography (CT), permit detailed imaging of complex parts [1], but can be slow and expensive. The lack of simple, reliable, and inexpensive methods for NDE of AM parts is a significant obstacle to their wider adoption.

Electromechanical impedance measurements have been investigated as a means to detect manufacturing defects in AM parts [2]. Impedance-based NDE utilizes piezoelectric wafers as collocated sensors and actuators. Taking advantage of the coupled electromechanical characteristics of piezoelectric materials, the mechanical characteristics of the part under test can be inferred from the electrical impedance of the piezoelectric wafer. Previous efforts have used piezoelectric wafers bonded directly to the part under test, which imposes several challenges regarding the applicability and robustness of the technique [2, 3].

This paper investigates the use of an instrumented clamp that can be temporarily affixed onto a part for measurement of its electromechanical impedance. Moving towards a mechanically attached solution would eliminate the need to wait for a bonding agent to cure, and would also address issues related to removing the sensor following testing. However, a mechanical

C. Tenney (✉)
Vibrations and Adaptive Structures Testing Laboratory (VAST), Design, Research & Education for Additive Manufacturing Systems (DREAMS) Lab, Virginia Polytechnic Institute and State University (Virginia Tech), Blacksburg, VA, USA
e-mail: charten@vt.edu

M. Albakri · P. Tarazaga
Vibrations and Adaptive Structures Testing Laboratory (VAST), Virginia Polytechnic Institute and State University (Virginia Tech), Blacksburg, VA, USA

C. B. Williams
Design, Research & Education for Additive Manufacturing Systems (DREAMS) Lab, Virginia Polytechnic Institute and State University (Virginia Tech), Blacksburg, VA, USA

S. Pakzad (ed.), *Dynamics of Civil Structures, Volume 2*, Conference Proceedings of the Society for Experimental Mechanics Series, https://doi.org/10.1007/978-3-319-74421-6_35

attachment mechanism makes the sensor larger and heavier, which could affect the sensitivity of the measurement. To address this potential issue, the effectiveness of this approach in detecting manufacturing defects is compared to directly bonded wafers.

In order to evaluate the use of the instrumented clamp, this paper proceeds as follows. First, a theoretical overview of impedance-based NDE is presented. Next, the design and fabrication of test specimens, instrumentation of the clamp and specimens, and the testing parameters are laid out. Then the results of testing are presented and analyzed. Finally, some concluding remarks and suggestions for future work are made.

35.2 Impedance-Based Non-destructive Evaluation

Impedance-based NDE examines the dynamic vibrational response of a test object and compares that response to some established baseline. The rationale for this comparison is that the changes in mass, stiffness, and damping that result from manufacturing defects will manifest as changes in the object's dynamic response, affecting the frequency and magnitude of the object's resonances.

Interrogation of the dynamic response is accomplished using piezoelectric transducers as collocated sensors and actuators. Since the mechanical and electric properties of a piezoelectric transducer are coupled, its electrical impedance can be related to the mechanical properties of the transducer and the object to which it is bonded. In this work, the piezoelectric transducer takes two forms: a macro fiber composite (MFC) patch that consists of lead zirconate titanate (PZT) strands adhered within two layers of polyimide film [4], as well as a monolithic PZT wafer.

Instrumenting the test object is done by bonding the piezoelectric transducer to a free surface, as shown in Fig. 35.1, then electrically exciting the transducer with an applied voltage. For the monolithic wafers, voltage applied through the thickness causes response in the 31 mode: electrical stimulus is applied in the thickness (3-direction), and strain is developed along the length (1-direction). In the MFC patch being used the response is in the 33-mode, but due to the orientation of the fibers and electrodes the excitation applied to the bonded surface is similar. For the monolithic wafer, we can solve analytically for the electrical impedance of the piezoelectric in terms of material properties and geometry. A similar derivation could be done for the MFC patch.

First, the constitutive equations for linear piezoelectricity that capture the 31 mode are shown in Eq. 35.1 [5]

$$\varepsilon_{11} = s_{11}^{E}\sigma_{11} + d_{13}E_3 \tag{35.1}$$

$$D_3 = \left(d^T\right)_{31}\sigma_{11} + \epsilon_{33}^{\sigma}E_3$$

where ε_{11} is the normal strain in the 1-direction, s_{11}^{E} is the complex elastic compliance constant measured at constant electric field, σ_{11} is the normal stress in the 1-direction, d_{13} and $(d^T)_{31}$ are piezoelectric constants, E_3 is the electric field strength in the 3-direction, D_3 is the charge displacement in the 3-direction, and ϵ_{33}^{σ} is the complex permittivity in the 3-direction measured at constant stress.

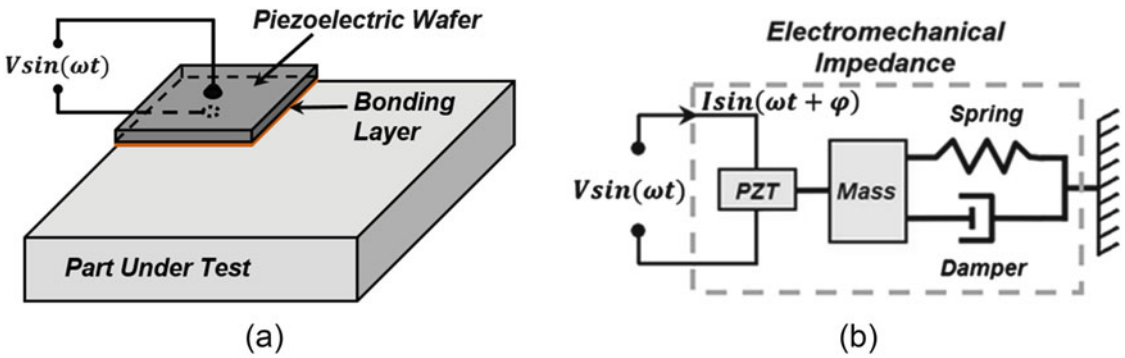

Fig. 35.1 (**a**) a piezoelectric transducer bonded to a test object, (**b**) an abstracted system diagram for the arrangement in (**a**) when excited at a particular frequency [3]

Table 35.1 Process parameters

Machine model	Stratasys Fortus 450mc	*Nozzle temperature*	355 °C
Model material	Stratasys Nylon 12	*Build chamber temperature*	120 °C
Support material	Stratasys SR-110	*Layer height*	0.01″ (0.254 mm)

For a test object, the dynamic response to excitation at any particular frequency can be approximated by a single degree of freedom system as shown in Fig. 35.1. The parameters of the system can be written m_r, k_r, and ζ_r, denoting mass, stiffness, and damping, respectively.

Then, assuming the piezoelectric transducer is perfectly bonded to the test object, Eq. 35.2 shows the electrical impedance of the transducer written in terms of the properties of the piezoelectric and of the test object [6, 7].

$$Z(\omega) = \left[i\omega \frac{bl}{h} \left(\frac{d_{11}^2}{s_{11}^E} \left(\frac{\tan(kl)}{kl} \left(\frac{Z_{pzt}}{Z_{pzt} + Z_{st}} \right) - 1 \right) + \epsilon_{33}^{\sigma} \right) \right]^{-1} \tag{35.2}$$

where $Z_{pzt} = -i\,(bh/l)\left(s_{11}^E \omega \tan(kl)/kl\right)^{-1}$ is the piezoelectric transducer impedance under short-circuit conditions, $Z_{st} = 2\zeta_r (k_r m_r)^{1/2} + i(m_r\omega^2 - k_r)/\omega$ is the mechanical impedance of the test object, $k = \omega\left(\rho s_{11}^E\right)^{1/2}$ is the wavenumber, ρ, b, h, and $2l$ are the piezoelectric density, width, thickness, and length, respectively.

In this study, a baseline impedance signature will be established, then compared to the impedance signature of a damaged test object. Differences between the two signatures will be interpreted as damage. This procedure has been carried out in many other studies, including the ones conducted by the authors of this paper [2, 3]. In order to quantitatively compare the signatures, Root-Mean-Square Deviation (RMSD) and the Correlation Coefficient (r) will be used as damage metrics. These metrics can be calculated using Eqs. 35.3 and 35.4.

$$RMSD = \sqrt{\sum \frac{(Z_D - Z_{BL})^2}{Z_{BL}^2}} \tag{35.3}$$

$$r = 1 - \left| \frac{n \sum Z_D Z_{BL} - \sum Z_D \sum Z_{BL}}{\sqrt{\left[n \sum Z_D^2 - \left(\sum Z_D \right)^2 \right] \left[n \sum Z_{BL}^2 - \left(\sum Z_{BL} \right)^2 \right]}} \right| \tag{35.4}$$

where Z_D is the impedance signature of the part being tested, Z_{BL} is the baseline impedance signature, and n is the number of data points in each impedance signature. As defined above, these metrics converge to zero when two signatures are identical, and increase as the signatures become less similar.

35.3 Test Specimen and Clamping Device Specifications

The test specimens used in this study, shown in Fig. 35.2, are rectangular beams measuring 72.5 × 7.25 × 5 mm, not including the 1 mm height of the L-shaped rails used to align the piezoelectric transducers. Each specimen is fabricated using a material extrusion additive manufacturing process (also referred to as "Fused Filament Fabrication", FFF). This process builds up a three dimensional structure by extruding filament through a heated nozzle. The machine model and process parameters can be found in Table 35.1. The part material, nylon, is intended to be representative of a common plastic type found in a range of polymer-based additive manufacturing (AM) processes. Additionally, the parts were fabricated with solid infill.

Following fabrication, the parts were post-processed by soaking them in a basic solution that dissolves the support material, according the material supplier's specifications. All support material had been removed after 2 h. Though it might have been preferable to fabricate the parts with no support material at all, the toolpath software for the Stratasys Fortus (Insight 10.1) automatically adds a raft of support material to every part. Finally, the parts were rinsed in fresh water, dried by hand, and then left to thoroughly air-dry for 24 h.

The clamping mechanism, shown in Fig. 35.2, used in this study is a small, metal, c-shaped clamp with a threaded rod that can be advanced to adjust the clamping force. The clamp fits within a volume of 105×65×60 mm when the threaded rod is retracted to minimize the height of the clamp. When fully extended, the clamp will accept an object with a height of approximately 73 mm.

In preparation for testing, an MFC patch was bonded to the clamp, and a monolithic PZT wafer was bonded to one of the beam specimens. On the clamp, a Smart Materials M-2814-P1 MFC patch was bonded using cyanoacrylate[1] to the base, as shown in Fig. 35.3. This MFC patch provides exposed soldering points to connect to the interior electrodes. On the side of the clamp, a strain gage was bonded similarly to monitor the strain due to bending. This strain will be used to infer and monitor the clamping force.

On the beam specimen, a 12.7 × 6.35 mm PZT-5H wafer was bonded using cyanoacrylate to the area defined by the L-shaped rails described previously. This can be seen in Fig. 35.4. The wafer's top and bottom surfaces are nickel-coated to serve as electrodes. This arrangement leaves one surface inaccessible after bonding the wafer to the beam. To allow access, a short section of copper tape with a conductive adhesive was applied to the wafer before bonding.

35.4 Experimental Setup

Two configurations are considered in this paper. The first will be referred to as the "bonded configuration": a monolithic PZT wafer is bonded directly to a beam specimen, and then the wafer-and-beam system is suspended by monofilament. The second will be referred to as the "mechanically attached configuration": an MFC patch is bonded to the clamping mechanism, an un-instrumented-beam is clamped within it, and then the whole assembly is suspended by monofilament. By suspending each configuration, a free boundary condition is simulated.

Once the beam specimens and the clamp had been instrumented, impedance signatures were taken, as shown in Fig. 35.4a. For both cases, the impedance signature was measured using a Keysight E4990A impedance analyzer: a device that precisely

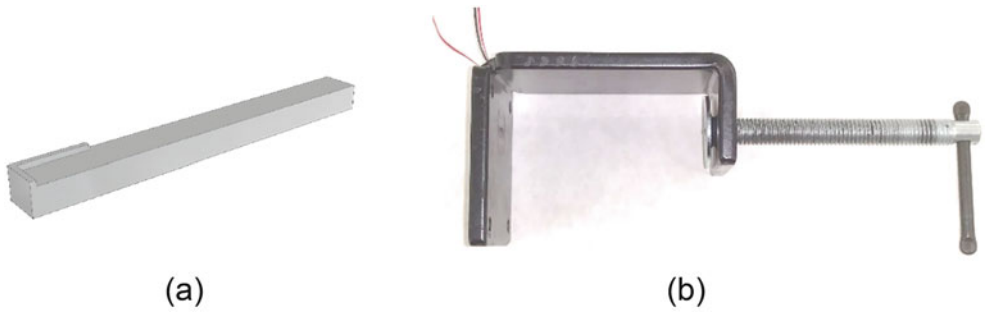

Fig. 35.2 (**a**) a rendering of a beam specimen, (**b**) the clamping mechanism

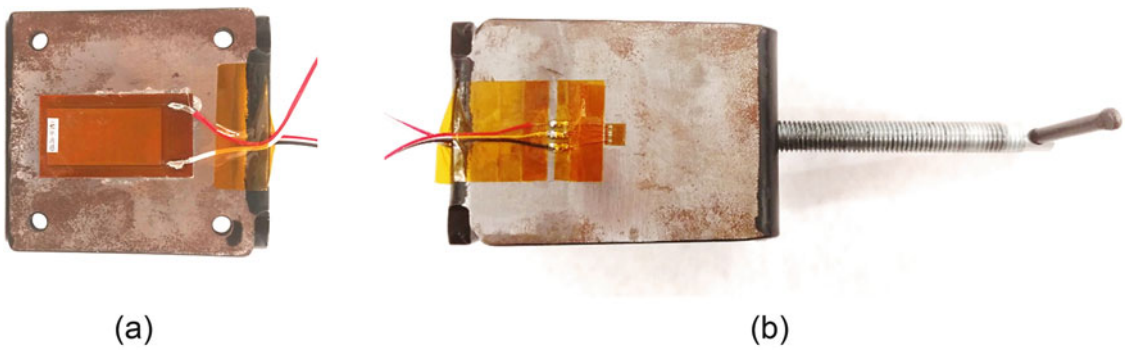

Fig. 35.3 (**a**) the MFC bonded to the bottom of the clamp, (**b**) the strain gage bonded to the side of the clamp

[1] Known by its trade name: Super Glue.

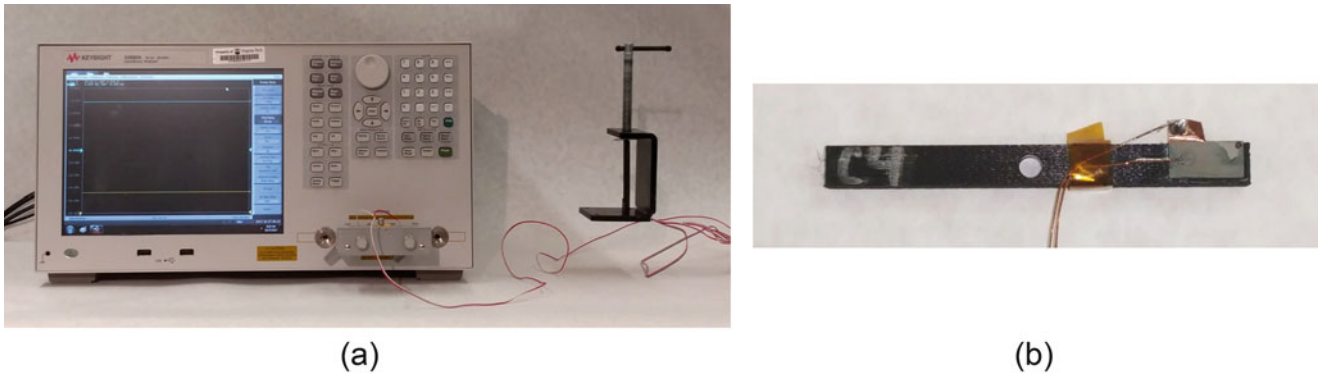

Fig. 35.4 (**a**) the suspended clamped beam specimen with the MFC patch connected to the impedance analyzer, (**b**) the free-beam with bonded PZT wafer (rectangle at right end) and damage applied (circle at center span)

delivers a voltage signal and measures current in order to determine electrical impedance. The signature was sampled at 1 Hz increments from 1000 Hz to 100 kHz. The excitation at each frequency was a 1 V peak-to-peak sinusoidal signal. Before taking each measurement, the excitation was applied to the test object to allow it time to settle. Without time to settle, the impedance signature has many peaks and troughs near any resonance of the system; a parsimonious explanation for this is that the shift from one frequency to the next was creating broadband excitation that needed to be damped out before the response at precisely one frequency could be accurately measured. For the mechanically attached configuration, it was observed that approximately 100–1000 ms was required to avoid spurious results, depending on the excitation frequency. The bonded configuration alone was observed to require only about 10 ms, presumably due to the higher damping of the plastic as compared to the metal of the clamp.

For the mechanically attached configuration, a Vishay 2110A strain gage conditioner was used to monitor the clamping force. The clamping force is relevant to the impedance signature because strains in a material affect the wave propagation speed within it, and therefore shift its resonant frequencies. The output gain of the conditioner was adjusted so that the output voltage matched the output of a force transducer being compressed by the clamp. A ball bearing was added to the end of the clamp's threaded rod in order to minimize contact area and thereby avoid torqueing the test object. For this study, the clamping force was initially adjusted to 150 N (34 lb), though over the course of testing this value fell to approximately 140 N (32 lb), possibly due to gradual deformation of the beam over hours.

35.5 Procedure

In this study, each beam specimen is being compared to itself: an impedance signature is recorded with the beam specimen in its defect-free state, then again after the application of damage. Because the specimen is being compared to itself—and because the impedance signature has been found to be repeatable over time [8]—a single measurement with the beam in its defect-free state is used as the baseline for comparison.

The damage applied to each beam specimen was made large due to account for the unknown damage-sensitivity of the instrumented clamp. In both the clamped and free configurations, the damage introduced was a drilled hole of diameter 3.9 mm, located equidistant from both ends of the beam as shown in Fig. 35.4b. After the damage had been applied, a second impedance measurement was taken.

35.6 Results and Discussion

In this section, the collected impedance signatures are presented and analyzed. First, the baseline measurements of the mechanically attached and directly bonded configurations are presented and regions of interest are identified. Then, the baseline and damaged signatures are compared.

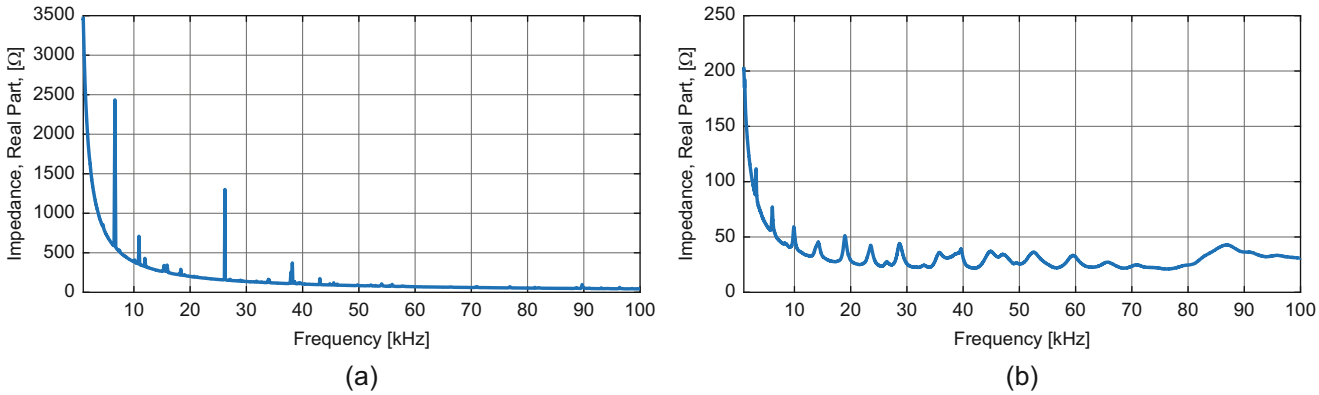

Fig. 35.5 The real part of the impedance signature for (**a**) mechanically attached and (**b**) directly bonded configurations

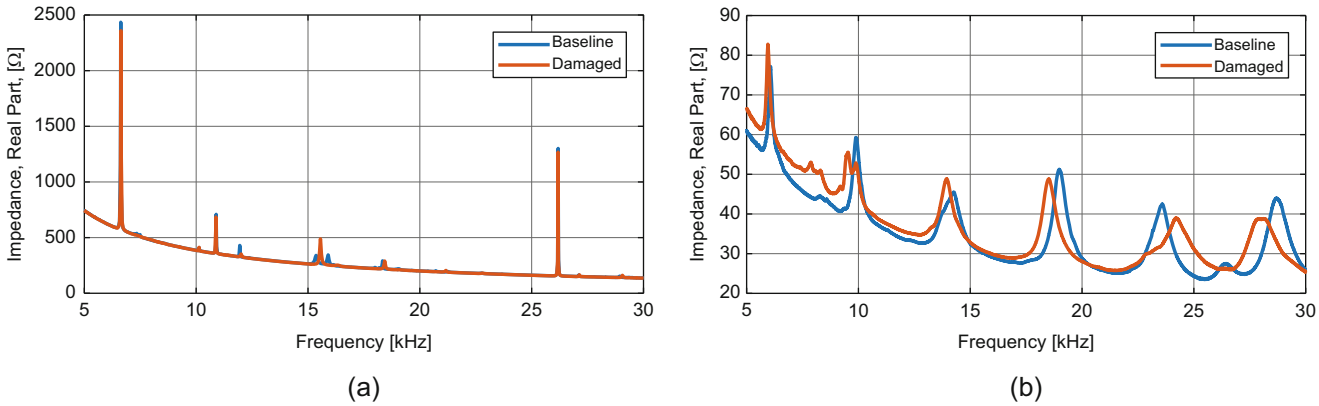

Fig. 35.6 Comparing baseline to damage: (**a**) the real part of the mechanically attached impedance signatures, and the same for (**b**) the directly bonded signatures

35.6.1 Baseline Measurements

A baseline is established by obtaining an impedance signature from damage-free specimens. In Fig. 35.5, the real part of the impedance signature for both the attached and bonded configurations are presented over the full frequency range measured (1–100 kHz). The qualitative response of each is similar: both have an overall decaying trend punctuated with peaks in similar frequency ranges. The individual peaks don't all align, since these are completely different structures. However, we should expect to see something of the beam's response in the response of the clamp-beam system.

Some major differences between the two plots can be attributed to the differences in the configurations. The difference in overall magnitude is due to the different piezoelectric transducers used in each test. The clamp was instrumented with an MFC patch while the beam was instrumented with a PZT wafer. Due to geometry and construction, the MFC has a greater magnitude response regardless of the structure to which it is bonded. The sharpness of the peaks is related to the damping of the structure; the sharp peaks of the mechanically attached configuration are consistent with a mostly-metal structure, while the rounded peaks of the bonded configuration are consistent with a more strongly damped, mostly-plastic system. Since both signatures are rich in peaks around the 5–30 kHz region, regions of interest will be drawn from this range.

35.6.2 Comparison to Damaged Specimens

Next, impedance signatures are obtained from the specimens after damage has been applied. In Fig. 35.6, the impedance signatures of the damaged attached-configuration and damaged bonded-configuration are compared to their respective baselines over the 5–30 kHz range described in the previous subsection.

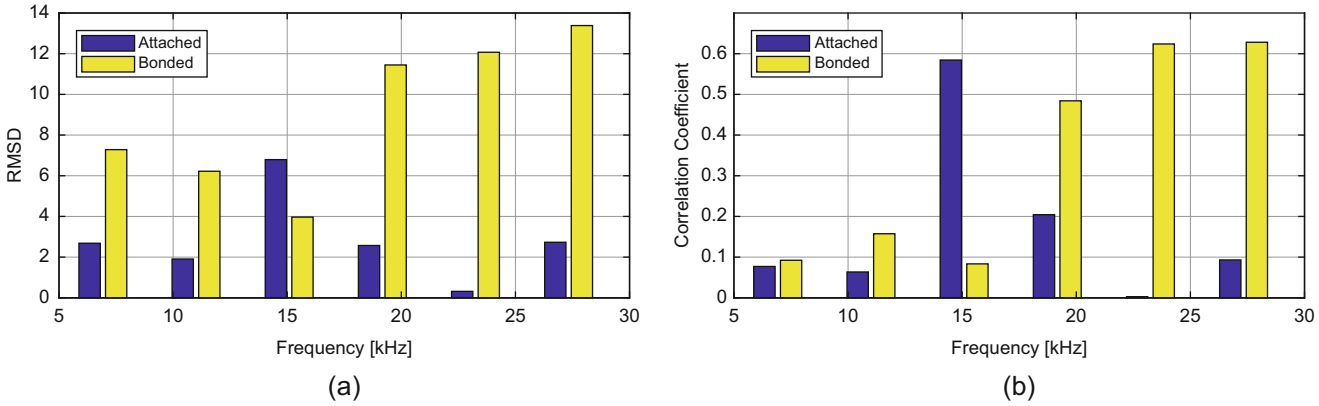

Fig. 35.7 Damage metrics calculated over the frequency range of interest: (**a**) RMSD, (**b**) correlation coefficient (r)

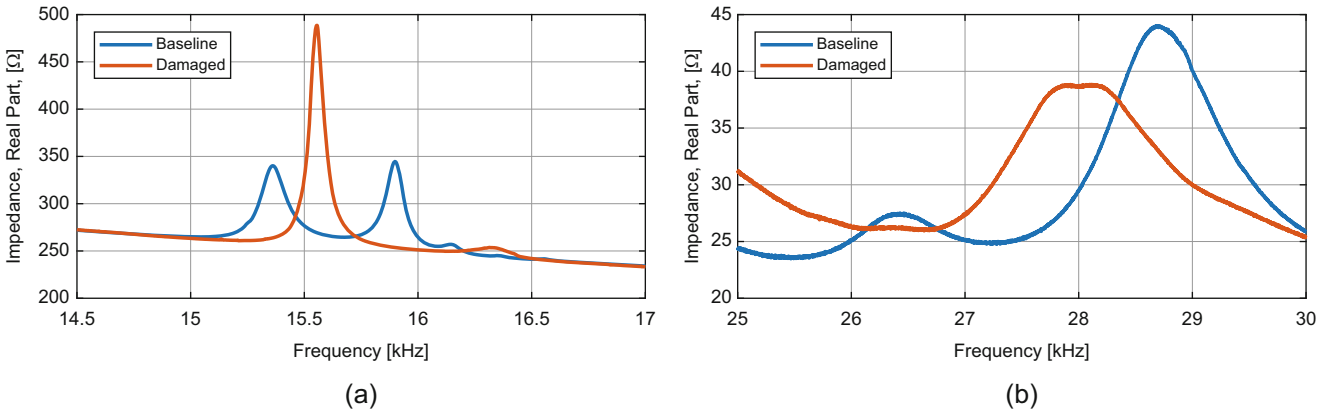

Fig. 35.8 Examining the regions with highest correlation coefficient damage metrics: (**a**) a range within the mechanically attached signature, and (**b**) a range within the directly bonded signature

Looking at the effects of damage application in each configuration, the bonded configuration shows a clear frequency shift across all peaks in the region. In the mechanically attached case, magnification is needed to clearly see the frequency shifting, provided later in Fig. 35.8. This is consistent with the fact that the damage introduced is much larger in comparison with the size of the bonded configuration—the beam alone—than in comparison to the attached configuration—beam and clamp together. Moreover, the transducer is both closer to the damage and more directly attached to the damaged object in the bonded configuration. But critically, in both cases, the damage can be clearly seen with appropriate magnification. In Fig. 35.7, the damage metrics described in Sect. 36.2 are calculated in 4 kHz bins for the frequency range of interest.

Another interesting result is the distribution of the damage throughout the signature. In the attached case, the damage metrics spike in one bin, while the damage is more evenly distributed throughout the range in the bonded case. This can be explained by considering the attached signature to be dominated by the dynamic response of the clamp. The damage to the beam specimen only affects the clamp if the particular mode of vibration is applying force through the beam. A torsional mode of the clamp or a bending mode in the bottom plate might have very low sensitivity to changes in the beam, for example. This is behavior that deserves further investigation. Figure 35.8 shows the range with the highest correlation coefficient damage metric in both configurations, to provide a point of comparison

Finally, in order to demonstrate the measurement repeatability of the impedance signature, an additional measurement was taken for the damaged specimens. The beam specimens used for the second measurement are the same specimens used for the first measurement in each configuration. In Fig. 35.9, the baseline is compared to the two damaged signatures for each configuration, and the damage metrics are calculated. By inspection of the impedance signature, it is clear which two signatures come from the post-damage case. Additionally, the damage metrics are much smaller than the values shown in Fig. 35.7, indicating a small amount of change. These small changes may be due to temperature variations, fatigue at the electrical contacts, or some other source, but they are small enough that they are easily distinguishable from the damage introduced above.

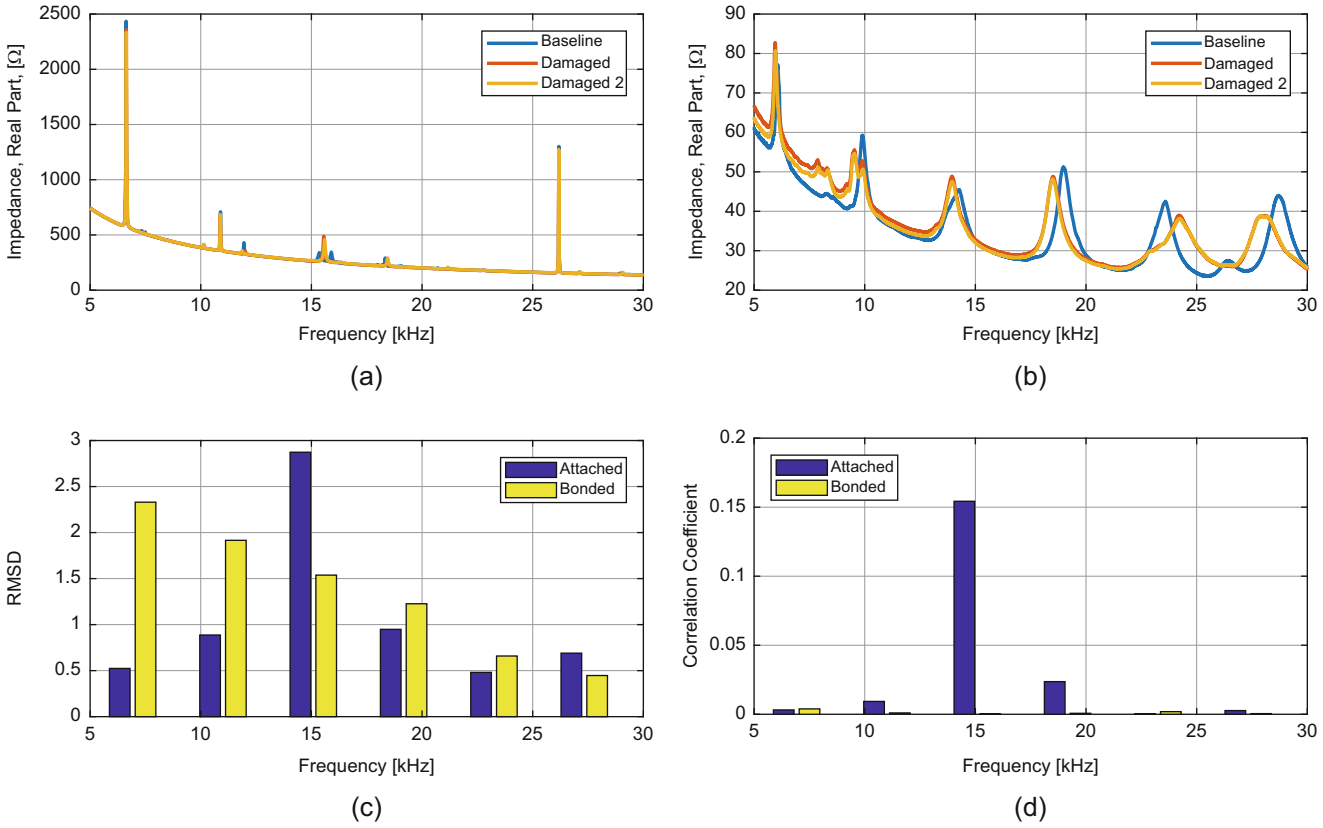

Fig. 35.9 Comparing a second damaged signature to the first. (**a**) impedance for the attached configuration, two damaged signatures plotted with one baseline, (**b**) the same for the bonded configuration, (**c**) RMSD values comparing 'Damaged' and 'Damaged 2' for each configuration, (**d**) correlation coefficient values comparing 'Damaged' and 'Damaged 2' for each configuration

35.7 Conclusions

In this paper, the plausibility of mechanically attached piezoelectric transducers for damage detection in AM parts is examined and compared to directly bonded transducers. The test specimens were rectangular beams, and damage was applied to the beams at mid-span for each of the two test configurations: directly bonded and mechanically attached. For both configurations, the electrical impedance of the attached/bonded transducer was measured over a 1–100 kHz range. Then, damage was applied and the measurement was repeated. Examining the measurements, it was found that both configurations had a dense area of resonant peaks in the 5–35 kHz range. For this range, root-mean-square and correlation damage metrics were calculated comparing the damaged measurement to the un-damaged measurement baseline.

By inspection of the impedance signatures and based on the values of the damage metrics, it was determined that both the mechanically attached and directly bonded configurations are capable of detecting damage to beam specimens at the scale employed in this work. However, it was noted that damage was registered at several resonant peaks in the bonded configuration, while fewer peaks clearly reflected the effects of damage for the attached configuration. This indicates that some resonances of the clamp are more sensitive to damage in the beam specimen than others.

Going forward there is much room for characterization of the effect of clamping orientation and force, as well as the effect of using specimens of different sizes, materials, and geometries. Overall though, mechanically attaching a specimen to an instrumented clamp is found to have potential as an alternative to directly bonding piezoelectric transducers for electromechanical impedance measurements.

35.8 Acknowledgement

This material is based upon work supported by the National Science Foundation under Grant Number CMMI-1635356. Any opinions, findings, and conclusions or recommendations expressed in this material are those of the author(s) and do not necessarily reflect the views of the National Science Foundation.

Additionally, the authors thank Joseph Kubalak for fabricating the beam specimens used in this paper, and for his help in accurately describing the process.

References

1. Du Plessis, A., Le Roux, S.G., Els, J., Booysen, G., Blaine, D.C.: Application of microCT to the non-destructive testing of an additive manufactured titanium component. Case Stud. Nondestruct. Test. Eval. **4**, 1–7 (2015)
2. Albakri, M.I., Sturm, L.D., Williams, C.B., Tarazaga, P.A.: Impedance-based non-destructive evaluation of additively manufactured parts. Rapid Prototyp. J. **23**(3), 589–601 (2017)
3. Tenney, C., Albakri, M., Kubalak, J., Sturm, L., Williams, C., Tarazaga, P.: Internal porosity detection in additively manufactured parts via electromechanical impedance measurements. In: Smart Materials, Adaptive Structures and Intelligent Systems. American Society of Mechanical Engineers, New York (2017)
4. Smart Material: Macro fiber composite (MFC) datasheet. p. 8, (2017)
5. Meitzler, A.H., Tiersten, H.F., Warner, A.W.: An American National Standard IEEE Standard on Piezoelectricity. IEEE, New York (1987)
6. Park, G., Sohn, H., Farrar, C.R., Inman, D.J.: Overview of piezoelectric impedance-based health monitoring and path forward. Shock Vib. Dig. **35**(6), 451–463 (2003)
7. Liang, C., Sun, F.P., Rogers, C.A.: Coupled electro-mechanical analysis of adaptive material systems-determination of the actuator power consumption and system energy transfer. J. Intell. Mater. Syst. Struct. **8**(4), 335–343 (1997)
8. Bhalla, S., Surendra, A., Naidu, K., Wee, C.: Practical issues in the implementation of electro-mechanical impedance technique for NDE. SPIE. **4935**, 484–494 (2002)